1   **Improved understanding of spatiotemporal controls on regional scale groundwater flooding using**

2   **hydrograph analysis and impulse response functions**

3

4

5   Ascott, M.J. [a], Marchant, B.P.[b], Macdonald, D.M.J. [a], McKenzie, A.A. [a] and Bloomfield, J.P. [a]

6   [a] British Geological Survey, Maclean Building, Crowmarsh Gifford, Oxfordshire, OX10 8BB, UK

7   [b] British Geological Survey, Environmental Science Centre, Nicker Hill, Keyworth, Nottingham, NG12

8   5GG, UK

9

10

11   Corresponding Author: Ascott, M.J.[*]

12   *British Geological Survey, Maclean Building, Crowmarsh Gifford, Oxfordshire OX10 8BB, UK.

13   matta@bgs.ac.uk, +44(0)1491 692408

14

15

16

17

18

19

20

21

22

Abstract

Controls on the spatiotemporal extent of groundwater flooding are poorly understood, despite the long duration of groundwater flood events and distinct social and economic impacts. We developed a novel approach using statistical analysis of groundwater level hydrographs and impulse response functions (IRFs) and applied it to the 2013/14 Chalk groundwater flooding in the English Lowlands. We proposed a standardised index of groundwater flooding which we calculated for monthly groundwater levels for 26 boreholes in the Chalk. We grouped these standardised series using k-means cluster analysis and cross-correlated the cluster centroids with the Standardised Precipitation Index (SPI) accumulated over time intervals between 1 and 60 months. This analysis reveals two spatially coherent groups of standardised hydrographs which responded to precipitation over different timescales. We estimated IRF models of the groundwater level response to effective precipitation for three boreholes in each group. The IRF models corroborate the SPI analysis showing different response functions between the groups. We applied identical effective precipitation inputs to each of the IRF models and observed differences between the hydrographs from each group. It is suggested this is due to the hydrogeological properties of the Chalk and of overlying relatively low permeability superficial deposits (recent unconsolidated sediments overlying the bedrock, such as clays and tills), which are extensive over one of the groups. The overarching controls on groundwater flood response are concluded to be a complex combination of antecedent conditions, rainfall and catchment hydrogeological properties. These controls should be taken into consideration when anticipating and managing future groundwater flood events. The approach presented is generic and parsimonious and can be easily applied where sufficient groundwater level and rainfall data are available.

Keywords:

48   Groundwater flooding, Chalk hydrogeology, impulse response functions, standardised precipitation

49   index, hydrograph analysis

1   Introduction

51

52   Flooding is estimated to affect more people globally than any other natural hazard, with an average

53   of 250 million people affected annually (United Nations Office for Disaster Risk Reduction, 2013). In

54   comparison to fluvial and pluvial flooding, flooding from groundwater has only recently been given

55   adequate consideration following groundwater floods in Northern and Central Europe in the past two

56   decades (Robinson *et al.*, 2001; Pinault *et al.*, 2005; Kreibich *et al.*, 2009; Macdonald *et al.*, 2012).

57   Groundwater flooding is the emergence of groundwater at the ground surface away from perennial

58   river channels or the rising of groundwater into man-made ground, under conditions where the

59   'normal' ranges of groundwater level and groundwater flow are exceeded (Finch *et al.*, 2004;

60   Macdonald *et al.*, 2008). Whilst groundwater flooding in some limestone terranes can be shortlived

61   (Bonacci *et al.*, 2006), a more common characteristic feature of groundwater flooding events is the

62   relatively long duration compared with fluvial flooding (Cobby *et al.*, 2009; Hughes *et al.*, 2011). As a

63   result, it can cause social disruption and economic impact that is distinct from fluvial floods. In

64   England, preliminary work has suggested that groundwater flooding may cause economic losses of

65   £530m per year, approximately 30% of total losses associated with flooding from all sources (ESI,

66   2016).

67

68   Due to the relatively recent recognition of flooding from groundwater, and the difficulty in separating

69   it from other forms of flooding, there has been limited reporting of the impact of large scale

70   groundwater flooding (Finch *et al.*, 2004). Globally there has been some reporting of approaches to

71   assess groundwater flood risk (e.g. Chebanov and Zadniprovska (2011); Gotkowitz *et al.* (2014); Fürst

72   *et al.* (2015); Naughton *et al.* (2015)) but the majority of the studies of this hazard have been in the

3

73   United Kingdom. Regional groundwater flooding in the south of the UK in the winter of 2000/1, and

74   further major flooding in 2003 and 2007 that also included a significant groundwater component, led

75   to legislation to assess and devise measures to address groundwater flood risk nationally. Work has

76   been undertaken to develop national scale groundwater emergence and susceptibility maps (Morris

77   *et al.*, 2007; McKenzie *et al.*, 2010) which has led to the development of groundwater flood risk maps

78   (ESI, 2016; JBA, 2016). These flood risk maps address the two main settings for groundwater flooding:

79   shallow permeable superficial deposits (recent unconsolidated sediments overlying the bedrock)

80   associated with large rivers; and unconfined bedrock aquifers. Groundwater flooding on the outcrop

81   of the Chalk aquifer in the southern and eastern UK, that is within the latter category, has been the

82   primary focus for research. Catchment scale understanding of groundwater flood risk here has been

83   gained through specific case studies (Adams *et al.*, 2010; Upton and Jackson, 2011; Morris *et al.*, 2015).

84   Detailed site-scale investigations into recharge processes within this fractured dual porosity-dual

85   permeability carbonate aquifer have also given insight into the processes controlling groundwater

86   flooding associated with water table rises (Butler *et al.* (2012) and references therein). In contrast to

87   recharge by diffuse matrix flow, rapid groundwater level changes following specific rainfall events

88   have been attributed to flow within saturated or partially saturated fractures (Lee *et al.*, 2006; Ireson

89   and Butler, 2011). Changes in groundwater levels have been shown to be highly non-linear and

90   controlled by rainfall event intensity, duration and antecedent soil moisture conditions. At the

91   regional scale, however, limited work has been undertaken to understand the controls on

92   groundwater flooding. The role of both catchment properties and climate in controlling regional scale

93   impacts of drought has been established (Peters *et al.*, 2003; Van Lanen *et al.*, 2013), with the first

94   quantitative analyses of the relative importance of these factors recently undertaken (Van Loon and

95   Laaha, 2015; Tijdeman *et al.*, 2016). In contrast, the controls on the spatiotemporal distribution of

96   groundwater flooding are poorly understood (Hughes *et al.*, 2011). Climate change has potential to

97   cause higher frequency and more severe rainfall events (Fowler and Ekström, 2009), and recent work

98   has suggested that groundwater flooding in the UK may be 4 times more frequent in 2040 – 2069

99   (Jimenez-Martinez *et al.*, 2016). Consequently, it is critical that the controls on the spatiotemporal

100   extent of groundwater flooding are better understood.

101

102   In this paper we present a methodology to improve the process understanding of groundwater

103   flooding at the regional scale. Applied to the Chalk outcrop in the English Lowlands (Folland *et al.*,

104   2015), we use a novel combination of statistical analysis of groundwater level hydrographs and

105   groundwater modelling using impulse response functions to assess the hydrometeorogical and

106   hydrogeological controls on groundwater flooding. The application uses multi-decadal groundwater

107   level time series from the Chalk aquifer in combination with data from a specific flood event in the

108   winter of 2013/14. The methodology presented is generic and can be applied elsewhere to develop

109   conceptual models of groundwater flooding and improve groundwater flood management.

110

2   Materials and Methods

111

112

2.1   Study Area

113

114

115   The study area used was the outcrop of the Chalk aquifer in the south east of England. The study area

116   is shown in Figure 1 in addition to the names and locations of the principal regions within the southern

117   Chalk (Wessex, South Downs, Chilterns and the North Downs (Allen *et al.*, 1997)). The Chalk is a soft

118   microporous limestone which underlies large areas of north-west France, Belgium and the south and

119   east of the UK. At outcrop it is overlain by a series of younger unconsolidated superficial deposits,

120   including Clay-with-Flints and glacial tills. The Clay-with-Flints is a reddish stiff sandy clay of relatively

121   low permeability (K_{median} = 0.27 m/day, standard deviation = 0.74, based on grain size distribution

122   analysis by Bricker and Bloomfield (2014)), ranging in thickness from 0.5 to 10 m (Klinck *et al.*, 1988).

123   Glacial tills in the study area are of low permeability but highly heterogeneous (K_{median} = 1.61 m/day,

5

124 standard deviation = 65.38 (Bricker and Bloomfield, 2014)). Tills can be up to 20 m in thickness in the

125 study area (Bricker and Bloomfield, 2014) and have been shown to inhibit recharge by up to 85%

126 (Klinck *et al.*, 1997).

127

128 Groundwater sources within the Chalk can be highly productive and the formation is a principal aquifer

129 in these regions, providing up to 70% of the public water supply in areas of the south east of the UK.

130 Groundwater flow occurs both within the Chalk matrix and through fractures; most of the

131 groundwater storage is derived from secondary porosity created by the fractures (Downing *et al.*,

132 1993). Many factors have contributed to the aquifer properties of the Chalk (Downing *et al.*, 1993).

133 The regional-scale pattern of transmissivity has a number of controls, including the structure of the

134 Chalk (Blundell, 2002) and periglacial erosion. Superimposed upon the general distribution are other

135 effects which sometimes result in high permeability (MacDonald and Allen, 2001): the concentration

136 of groundwater flux within valleys; the lithology of the Chalk, especially the presence of marl layers,

137 flints or hardgrounds; the local structure of the Chalk, especially where significant fracturing has

138 developed; and younger cover, which can be instrumental in focusing recharge and developing

139 solution features and groundwater conduits. The high fracture permeability and relatively low storage

140 of the Chalk gives rise to comparatively large seasonal water table variations and associated stream-

141 head migration up dry valleys. Groundwater levels can vary significantly within the Chalk under normal

142 conditions. In the interfluves, where the unsaturated zone can be over 100 metres in thickness, the

143 difference between the minimum (October/November) and maximum (March/April) groundwater

144 levels can be tens of metres.

145

146 Research undertaken on recharge processes within the Chalk aquifer, particularly in relation to

147 groundwater flooding, has shown that the trigger point for groundwater flooding is the critical

148 saturation of the unsaturated zone (Adams *et al.*, 2008). When recharge occurs and critical saturation

149   is reached, a rapid rise in groundwater levels consequently occurs. During extreme recharge events

150   the associated rise in groundwater can result in flow in high permeability horizons of the Chalk,

151   resulting in groundwater appearing at the ground surface.

152

2.2   2013/14 Flood Event in southern UK

153

154

155   This study used the flood event in the UK that occurred in the winter and spring of 2013/14.

156   Substantial work has been undertaken to report the hydrological impacts (Kendon and McCarthy,

157   2015; Muchan *et al.*, 2015) and assess both the climatic and human influences on the

158   hydrometeorology of the event (Huntingford *et al.*, 2014; Davies, 2015; Huntingford *et al.*, 2015; van

159   Oldenborgh *et al.*, 2015; Schaller *et al.*, 2016). However, no regional scale reporting of the impacts

160   and causes of specific groundwater flooding during the event has been undertaken to date. Between

161   mid-December 2013 and mid-February 2014, a succession of low pressure systems crossed the UK,

162   resulting in its wettest winter on record (Kendon and McCarthy, 2015). The persistent heavy rainfall

163   meant that the winter was distinctive for the occurrence of pluvial, fluvial, and groundwater flooding

164   in southern and central England, as well as coastal flooding in the far southwest caused by the strong

165   winds, high tides and storm surges. The relative importance of these different types of flooding varied

166   geographically and over the course of the winter, but it was particularly notable for the exceptional

167   duration of flooding from both surface and groundwater in the River Thames valley and groundwater

168   flooding on the Chalk outcrop.

169

170   At the start of December 2013, flows in most rivers across the UK were in recession and river

171   discharges were below the seasonal average. Groundwater levels in the Chalk were in the normal

172   range or below. However, from mid-December onwards these recessions were interrupted by sharp

173   river flow and groundwater responses to the onset of the storms, particularly in southern England.

174   Water level rises of over 25 m were recorded during December in some boreholes and the first

175   groundwater flood alerts were issued on 26 December 2013. By the end of January, record monthly

176   levels had been recorded at six out of the 11 Chalk boreholes in southern England used to assess the

177   status of groundwater nationally (Muchan *et al.*, 2015). Extensive groundwater flooding occurred

178   across this region during February impacting both property and infrastructure. By the end of April,

179   Chalk water levels were falling throughout the country, however, levels remained exceptionally high

180   in some areas until June with localised flooding continuing throughout the spring and early summer.

181   There were isolated incidences of sewers continuing to surcharge, basements still being pumped and

182   minor roads remaining submerged into July (Muchan *et al.*, 2015).

183

184   The floods during the winter of 2013/14 in the UK caused widespread disruption, damage to property

185   and infrastructure (Ascott *et al.*, 2016) and a number of deaths. Total economic damages for England

186   and Wales associated with the floods have been estimated at between £1 and 1.5 billion (Environment

187   Agency, 2016). Figure 2 shows the impact of the flood event as indicated by the length (days) of flood

188   alerts for groundwater issued by the environmental regulator (n.b. all groundwater flood alert zones

189   in England are associated with the Chalk aquifer), flood-related travel alerts and media reports of

190   flooding, both of which were located on the Chalk outcrop and assumed to be due to groundwater

191   emergence. We scraped travel alerts and media reports from the British Broadcasting Corporation

192   (BBC) national and local news web sites every 3 days from 4th January 2014 to 22nd April 2014. Data

193   were published as JavaScript Object Notation (JSON), an easily read data-interchange format that

194   included the date the alert was first issued, latitude, longitude, cause and severity. Total winter rainfall

195   (Tanguy *et al.*, 2016) was heaviest across the southern and western areas of the Chalk outcrop.

196   Significantly less rain fell in the Chilterns to the north of the Chalk outcrop. This rainfall distribution is

197   reflected in the impact data. There were significantly more groundwater flood alerts in the South

198   Downs and Wessex areas than in the Chilterns. The travel alerts and media reports also broadly reflect

199   the impact of the rainfall patterns, with more travel alerts in the southern and western Chalk than in

200   the northern area.   The lack of groundwater flood impacts in the Chilterns during the 2013/14 flood

201   event is in contrast to previous events such as winter 2001, when substantial groundwater emergence

202   occurred in the northern area (Robinson *et al.*, 2001).

203

204   ## 2.3   Hydrograph Analysis
205

206   We developed a standardised index for groundwater flooding based on the Standardised

207   Groundwater Level Index (SGI) (Bloomfield and Marchant, 2013; Bloomfield *et al.*, 2015). The SGI is a

208   normalised and de-seasonalised index showing the variation in groundwater levels relative to the

209   seasonal norm. It is derived from long-term time series (typically longer than 30 years) of regularly

210   sampled groundwater levels from a single borehole. Bloomfield et al. (2015) apply the SGI to a time

211   series of groundwater levels from boreholes that are sampled every month. Each calendar month is

212   treated separately and the quantiles of the empirical distribution of groundwater levels are

213   determined and each groundwater level is transformed to the corresponding quantile of a

214   standardised (zero mean and unit variance) normal distribution. These 12 standardised series are then

215   merged to produce the SGI. The SGI was inspired by the Standardised Precipitation Index (SPI; (McKee

216   *et al.*, 1993)) although precipitation data are usually accumulated over a number of months before

217   calculating the SPI, and a parametric (e.g. gamma) model of the data distribution from a calendar

218   month is used rather than the empirical, non-parametric distribution.

219

220   We modified the SGI in two ways so that it could be used to focus on floods rather than the entire

221   groundwater hydrograph. First, rather than considering each calendar month separately, we applied

222   the normalisation to the entire set of groundwater level measurements. Thus, the index reflected the

223   absolute rather than de-seasonalised groundwater level since incidences of groundwater flooding are

224 related to the absolute level of groundwater. Second, we set all negative normalised values to zero to

225 focus upon periods where the groundwater levels were higher than their median. This was done since

226 non-linear relationships between precipitation and groundwater levels have previously been

227 documented by Eltahir and Yeh (1999) and we are specifically interested here in the nature of possible

228 correlations between precipitation and incidences of flooding associated with high groundwater

229 levels. We refer to this modified index as the Standardised Groundwater Flood Index (SGFI). Figure 3

230 shows the groundwater level hydrograph, SGI and SGFI for a representative borehole in the Chalk

231 aquifer (Figure 4). We applied this SGFI methodology to monthly groundwater levels recorded in

232 boreholes in the southern Chalk aquifer (see Figure 1) between January 1980 and September 2014.

233 This time interval is sufficiently long to estimate the SGFI and includes the 2013/14 flood. We

234 restricted our analysis to hydrographs from 26 boreholes where there were fewer than 20% missing

235 values, no more than 12 successive missing values and no more than five missing values after January

236 2013. For these 26 hydrographs, the missing values were estimated by linear interpolation. The SGFI

237 values are likely to be inaccurate during prolonged periods of missing data but these isolated episodes

238 did not unduly effect our analyses of the underlying drivers of SGFI variation.

239

240 To identify similarities in the standardised Chalk groundwater hydrographs that might reflect key

241 physical controls on their response to rainfall, we performed a non-hierarchical k-means clustering

242 (Webster and Oliver, 1990) on the SGFI time series. This algorithm divides the hydrographs into k

243 groups to minimize the sum of the Euclidean distances between the monthly SGFI values for each

244 borehole and the SGFI centroid (average) of the group to which the borehole is allocated. The choice

245 of the number of clusters is somewhat subjective and so we repeated the clustering for k = 2 to k =

246 5.   To identify the appropriate number of clusters we adopted a parsimonious approach building on

247 the criteria developed by Bloomfield *et al.* (2015). Bloomfield *et al.* (2015) developed a rule-based

248 approach to identify the smallest number of clusters of hydrographs that resolved the spatial

249   distribution of the three aquifers in their study area. Using expert hydrogeological knowledge, we

250   selected the smallest value of k which gave an acceptable cluster partition which is consistent with

251   the regional scale spatial variation of flood characteristics in the Chalk. We examined the centroid or

252   mean of the SGFI for each cluster to assess the significance of the 2013/14 groundwater flood event

253   in the context of the 35 year Chalk groundwater level record used within this study.

254

255   We then considered the relationship between rainfall and groundwater levels within the different

256   clusters. We calculated the SPI for the average monthly precipitation time series (derived from Tanguy

257   *et al.* (2016)) in each cluster and attempted to identify easily calculable metrics that could be used to

258   replicate the partitioning of the boreholes. Previously, Bloomfield and Marchant (2013) demonstrated

259   that two such metrics could be used to distinguish different patterns of variation in the SGI. These

260   were $m_{\max}$, the range of significant (p=0.05) temporal autocorrelation in each SGFI series and $q_{\max}$,

261   the accumulation period of the SPI which led to the largest correlation with SGI. We calculated these

262   metrics for each borehole's SGFI and the centroid of each cluster. When calculating $q_{\max}$, we

263   determined the SPI for the monthly precipitation time series (derived from Tanguy *et al.* (2016)) using

264   accumulation periods of between 1 and 60 months. We then calculated the correlations between

265   these SPI series and both the individual SGFI time series and the cluster's SGFI centroid. The SPI series

266   were also shifted backwards by between 0 and 5 months to reflect the potential lag before

267   precipitation affects the groundwater level in the borehole. Bloomfield and Marchant (2013) had

268   found that this lag did not exceed 2 months for the UK boreholes that they considered. We recorded

269   the accumulation period, $q_{\max}$, and lag shift, τ, which led to the largest correlation between the SPI

270   and the SGFI. The zeroed SGFI values were included when calculating these correlations. Larger

271   correlations would have resulted if these zeroed values had been removed but this could lead to

272   misleading results since instances where the SPI was substantially greater than zero but the

273   groundwater levels were below the seasonal norm would not lead to a reduction in the correlation.

274

275   We then repeated the cluster analysis with m_{max} and q_{max} as variables, using the value of k identified

276   from the SGFI time series clustering. The cluster partition using the different variables was then

277   compared. This approach can be interpreted as the estimation of a simple model of the temporal

278   variation of SGFI for each group. However, our aim is to identify simple metrics and a more accurate

279   model could possibly be derived by using actual rather than de-seasonalised precipitation series and

280   by incorporating factors such as potential evapotranspiration and soil moisture into the model. The

281   simple model assumes that an SGFI value for a specific month is proportional to the standardised

282   precipitation accumulated over q_{max} months and delayed by τ months. The values of the q_{max} and τ

283   parameters are likely to be controlled by the particular hydrogeological properties relevant to the

284   group of boreholes.

285

2.4   Groundwater Modelling using Impulse Response Functions
286
287

2.4.1   Model development
288
289

290   The m_{max}, q_{max} and τ parameters described above are an accessible but overly simplistic description

291   of the hydrological controls on SGFI. To understand better the spatial variation in groundwater levels

292   and the relative influence of rainfall and local hydrogeological characteristics we estimated impulse

293   response functions (IRFs) for individual boreholes. An IRF describes the system response (in this case

294   changing groundwater levels) to a single unit of input (in this case effective precipitation) as a function

295   of the time since the input occurred. We define effective precipitation to be the observed

296   precipitation (derived from Tanguy *et al.* (2016)) minus the potential evapotranspiration (derived

297   from the Met Office Rainfall and Evapo-transpiration Calculation System (MORECS; (Hough and Jones,

298   1999)). von Asmuth *et al.* (2002) demonstrated that the Pearson Type III distribution:

$$\theta(t) = A \frac{a^s t^{s-1} \exp(-at)}{\Gamma(s)} \tag{1}$$

299

300 (where A, a and s are parameters, $\Gamma(s)$ is the gamma function of order s, and t is the shifted time

301 since the precipitation occurred) could adequately represent the groundwater level IRF. The function

302 is sufficiently flexible to permit different rates of initial increase in groundwater level over time as

303 water arrives in the saturated zone and then decrease as it is discharged. Then, y_i, the groundwater

304 level at time i can be calculated from:

$$y_i = \mu + \sum_{t=0}^{n} \theta(t) x_{i-t} \tag{2}$$

305

306 where μ is a fourth parameter of the model, n is the number of months considered in the IRF and x_i

307 is the effective rainfall at time i. We selected three boreholes for each of the groups identified by the

308 cluster analysis. The boreholes cover the majority of the spatial distribution of the clusters (Figure 4)

309 and are used for monthly hydrological reporting and forecasting (Hannaford *et al.*, 2014; Mackay *et*

310 *al.*, 2015). They are known to have minimal impacts of groundwater abstraction and no significant

311 surface water influence (Mackay *et al.*, 2015). Chilgrove House, Rockley, Stonor Park, West

312 Woodyates Manor are all located < 5 km from a groundwater flooding alert area. Well House Inn and

313 Therfield Rectory are located 10 and 66 km from a groundwater flooding alert area respectively. We

314 estimated Pearson Type III IRFs (for *t*=0 to 30 months) for the monthly groundwater response to local

315 effective precipitation for each of these boreholes by a least squares approach (von Asmuth et al.,

316 2002). We examined the shape of the modelled IRFs for each of the sites in the context of the SPI-

317 SGFI cross correlation analysis. For each of the sites we derived the percentage of Clay-with-Flints and

318 till cover for the surface catchments within which the boreholes are situated (as defined by Water

319 Framework Directive River Waterbody Catchments Cycle 2; Environment Agency (2015)).

320

2.4.2   Application using homogeneous rainfall inputs

322

323   As illustrated in Figure 2, the rainfall distribution during the 2013/14 flood event was highly spatially

324   variable, with total winter rainfall (December 2013 – April 2014 inclusive) ranging from < 400mm in

325   the Chilterns to > 1000 mm in Wessex. To quantify the relative significance of spatial heterogeneity

326   in rainfall and catchment hydrogeological properties in controlling groundwater level responses, the

327   same effective precipitation input was applied to all the IRFs from each of the clusters. The effective

328   precipitation time series for Chilgrove House (Figure 4) as calculated from Tanguy *et al.* (2016) and

329   MORECS (Hough and Jones, 1999) and used as the homogeneous input. The length of time

330   groundwater levels were above the 95th percentile level was used as a metric for flood persistence.

331   This metric was calculated for each site using the observed groundwater level data for the 2013/14

332   flood event and using the IRF models using both the site-specific rainfall and the spatially

333   homogeneous (Chilgrove House) rainfall input. The constant threshold value approach to defining

334   persistence is conceptually simple but the choice of percentile may be somewhat subjective

335   (Yevyevich, 1967). The 95th percentile has been used extensively in analysis of extreme rainfall events

336   (Christensen and Christensen, 2003) in addition to inland (Pirazzoli *et al.*, 2006) and coastal flooding

337   (Wu *et al.*, 2012). Published flood alert levels for groundwater used by the environmental regulator

338   for two of the IRF model sites (Figure 4) are consistent with this approach (Stonor - 96th percentile,

339   South Oxfordshire District Council (2016) and Chilgrove House - 95th percentile, CH2MHill (2015)).

340

3   Results

3.1   Hydrograph Analysis

343

344   The cluster analysis on the SGFI time series was conducted for $k = 2$ to $k = 5$. The clusters for $k = 2$

345   (shown in Figure 4) were considered to best reflect the large scale regional variation of groundwater

346   flood behaviour in the Chalk. The clusters for $k = 2$ are spatially coherent and patterns of cluster

347   membership for larger k were spatially irregular. Whilst cluster membership for $k > 2$ may reflect

348   local scale hydrogeological processes, this is not the focus of the regional scale approach developed

349   here to understanding large-scale controls on groundwater flooding. The Group 1 cluster is primarily

350   located in the south and west of the study area (Wessex and the South Downs, Figure 2) where the

351   Chalk is generally present at the ground surface or overlain by permeable superficial gravels. Group

352   2 is primarily located in the north and east (Chilterns, Figure 2), where substantial Clay-with-Flints and

353   Till are present (Figure 4). The SGFI time series for each cluster and the centroids are shown in Figure

354   5. The groups and their standardized groundwater level series can be characterised as follows:

355   •   Group 1 – groundwater levels are flashy, rising and recessing rapidly in response to recharge

356   events. The highest groundwater levels across the full period analysed occurred in the

357   2013/14 flood.

358   •   Group 2 – groundwater levels are slow both to rise in response to recharge and to

359   subsequently recess, sustaining high and low levels for longer periods of time compared with

360   the other group. Several multi-year periods are evident where the SGFI remains greater than

361   zero (for example, between 2001 and 2003). The highest groundwater levels occurred in the

362   2000/01 flood.

363

364   When undertaking k-means clustering for $k = 2$ on m_{max} and q_{max}, very similar cluster partitions were

365   achieved. In each case one borehole (on the geographical boundary between the two groups) was

366   allocated to the other group from its allocation in the SGFI clustering.   Figure 6 and Figure 7 show

367   distributions of m_{max} and $q_{\max}$ for each SGFI cluster. Boreholes in Group 2 have a significantly longer

368   memory and accumulation period than Group 1. When we explored the relationship between SPI and

369   the SGFI (Figure 8), we found that in Group 1 the two indices are most strongly positively correlated

370 when rainfall is accumulated over 5 months, whereas for Group 2, the optimal accumulation period is

371 16 months.

372

3.2 Impulse Response Function Modelling

374

375 Figure 9 and Figure 10 show the IRFs and modelled groundwater levels derived for the three boreholes

376 from Group 1 and 2 respectively. The shape of the IRFs corroborates the cross correlation analyses

377 presented in section 3.1, with the IRFs for boreholes in Group 2 remaining greater than zero for a

378 longer period than the IRFs from Group 1. The modelled groundwater levels are generally in good

379 agreement with observed levels (based on Nash and Sutcliffe Efficiency, see Table 1). The model

380 calibration appears to be slightly poorer in Group 2, particularly at Therfield Rectory where the IRF

381 model does not match the observed peaks in groundwater levels.

382

383 Table 1 shows the extent of Clay-with-Flints and till within each catchment (%CWF and TILL), the range

384 of significant temporal autocorrelation (m_{max}) for each borehole and the ratio of the total winter site

385 rainfall to the rainfall at Chilgrove House. Boreholes in Group 2 have a significantly longer "memory"

386 and greater amount of clay and till cover than those in Group 1. The number of months for each site

387 when observed groundwater levels were over the 95th percentile level during the 2013/14 flood event

388 is shown. Also presented is the modelled number of months over 95th percentile using both the site-

389 specific rainfall and the Chilgrove House rainfall, the homogenous rainfall input. There is a relatively

390 small discrepancy between the observed and modelled number of months over 95th percentile using

391 the site specific rainfall (mean absolute error = 2.8 months), with the exception of Therfield Rectory

392 where the difference is 14 months. The poor calibration achieved for this site and large discrepancy

393 between modelled and observed time over the 95th percentile limits the predictive ability of the

394 simplified IRF model at Therfield Rectory when using other rainfall inputs. Consequently, the decrease

16

395   in modelled number of months over the 95th percentile when using Chilgrove House rainfall from 16

396   to 12 months is likely to be inaccurate.

397

398   By using the Chilgrove House rainfall at Well House Inn and Stonor, the length of time where

399   groundwater levels are over the 95th percentile increases substantially by up to 11 months.   It should

400   be noted that the number of months over the 95th percentile also changes at the other boreholes in

401   Group 1 by 1 month. This is likely to be due to spatial variability in rainfall within the Group 1 cluster

402   during the 2013/14 flood event. This can be observed in both Figure 2 and the variability in the ratio

403   of total winter rainfall at Chilgrove House to the site-specific data (Table 1). The average number of

404   months over 95th percentile using homogeneous rainfall inputs is greater in the Group 2 cluster (12

405   months) than in Group 1 (7 months).

406   **4   Discussion**
407

408   **4.1   Insights into spatiotemporal controls on groundwater flooding**
409

410   The cluster analysis highlights clear spatial differences in the groundwater level response during a

411   flood event. Sites in Group 2 respond slower to rainfall inputs with greater lag between rainfall and

412   groundwater levels compared to sites in Group 1.   As previously discussed, one of the primary

413   differences in the hydrogeology of the two cluster areas is the extent of low permeability superficial

414   cover overlying the Chalk. As illustrated in Table 1 and Figure 4, in the Chilterns (Group 2), the Chalk

415   is extensively overlain by the Clay-with-Flints and till in the north of the study region. Bloomfield *et*

416   *al.* (2009) and Bloomfield *et al.* (2011) previously showed the role of these relatively low permeability

417   superficial deposits in Chalk catchments in influencing baseflow. We postulate that these deposits act

418   to slow and attenuate the recharge signal and so cause groundwater levels to rise and fall more slowly

419   in catchments where they are present. This effect may be enhanced in catchments where Clay-with-

17

420   Flints predominate since these deposits form over high ground and are typically associated with

421   relatively thick unsaturated zones, adding further to the potential for attenuation of recharge signals.

422   This is reflected in both the standardized groundwater level responses and the IRFs for the different

423   clusters.

424

425   As illustrated in Figure 2, the spatial extent of groundwater flooding that occurred during the 2013/14

426   event was controlled predominantly by the rainfall distribution. This is also reflected in the SGFI

427   centroids (Figure 5), with greater SGFI values during the 2013/14 flood event in Group 1. This spatial

428   variability in the rainfall input (<400 mm to >1000 mm over the study area for December 2013 – April

429   2014 inclusive) limits the direct use of the standardized groundwater level series for regional-scale

430   spatial analyses of groundwater flooding. By applying a spatially coherent rainfall input to IRF models

431   for boreholes within the two clusters, we have demonstrated that for a hypothetical scenario where

432   a uniform rainfall input occurred and raised groundwater levels, the temporal response in Group 2

433   would be longer than Group 1. If such an event caused groundwater flooding, this may have lasted

434   longer in Group 2 than Group 1. This shows that the controls on groundwater flooding are a complex

435   combination of antecedent conditions, rainfall inputs and Chalk and superficial deposit hydraulic

436   properties. This corroborates recent work which has shown that hydrological response to droughts is

437   a function of catchment characteristics as well as driving meteorology (Van Lanen *et al.*, 2013; Van

438   Loon and Laaha, 2015). However, in the case of floods, the relative importance of meteorology and

439   catchment controls is likely to be weighted towards the former due to the strong spatial variability in

440   rainfall inputs in comparison to drought events. This is highlighted by the variability within the clusters

441   of both rainfall and time over 95th percentile using the Chilgrove House rainfall (Table 1). Additional

442   local-scale hydrogeological processes (e.g. Chalk lithology, location of hardgrounds and faulting) not

443   considered in this regional analysis are also likely to exert controls on the spatiotemporal extent of

444   groundwater flooding.

446 The insight into spatiotemporal controls on groundwater flooding has significant implications for flood

447 management. The variability in the groundwater level response to rainfall inputs across the Chalk

448 implies that early warning systems and measures to address groundwater flooding must be developed

449 at a level below the aquifer scale. This is the case in England where the groundwater alert system

450 operated by the environmental regulator is focussed on a series of small catchments known to be

451 susceptible to groundwater flooding.

452 The understanding gained through this study does show that the interpretation of the groundwater

453 level hydrographs used within groundwater flood early warning systems and response plans must take

454 into account the catchment geology. In the Group 1 area of Wessex and the South Downs emergency

455 responders should anticipate relatively rapid onset when antecedent and ongoing rainfall conditions

456 make groundwater flooding likely. In the Group 2 area of the Chilterns, a relatively slow rise in

457 groundwater levels in the early warning boreholes should not be misinterpreted as meaning

458 groundwater flooding will not occur. However, when flooding does occur, response plans should

459 anticipate that this could persist for longer periods than may have been experienced in other areas.

460 Although local responders may be aware of the characteristics of local groundwater flood incidents,

461 an appreciation of the spatial variability in groundwater floods at a national level is important during

462 major regional events.

4.2 Standardized groundwater levels and impulse response function modelling for groundwater flood characterisation: an evaluation and outlook

466 In this study we have presented the first application of a methodology to explore the controls on

467 groundwater flooding which utilizes both statistical analysis of standardized hydrographs and IRF

468 modelling. The approach presented is generic and can be easily applied where long term groundwater

469 level and rainfall time series are available. Clustering of groundwater hydrographs has been

470 undertaken before (Upton and Jackson, 2011), however, such statistical analyses have never been

471   applied at the regional scale and in conjunction with IRF modelling. A distinct advantage of the

472   approach presented here over conventional models is the parsimony of the model parameterisation.

473   The IRF method consists of only four model parameters, whereas even relatively simple lumped

474   parameter models can include up to 16 (Marchant *et al.*, 2016). Whilst the model parameterisation

475   can be related to physical aquifer properties (Mackay *et al.*, 2014), often such parameters are

476   uncertain or unknown.

477

478   As previously discussed, groundwater flooding is difficult to distinguish from surface water flooding

479   and consequently understanding of the spatial and temporal extents of groundwater flooding is

480   generally poor. The approach presented here could form part of an exploratory analysis to assess the

481   likely variation in the temporal response in groundwater levels during a flood event. Assessment of

482   how the lag between standardized groundwater levels and SPI (Figure 8) varies between different

483   clusters of boreholes could help water managers develop appropriate strategies for managing future

484   groundwater flood events at the regional scale.

485

486   The 95th percentile threshold methodology provides a consistent approach to compare persistence of

487   high groundwater levels across different boreholes. However, it should be noted that estimates of

488   time above threshold have not been directly linked to observations of groundwater flooding. The

489   groundwater level in an early warning borehole at which groundwater flooding occurs that has a

490   societal impact is likely to be highly site specific, and related to an absolute level rather than a

491   percentile. Moreover, as flood events occur in the future and the length of record increases, the 95th

492   percentile will change, whilst absolute flooding thresholds will not. Absolute thresholds for riverine

493   flooding are well established as a result of historic recording of river flood events. In contrast, the

494   very limited observational records of groundwater emergence make defining absolute thresholds for

495 groundwater flooding highly challenging. Further data collection is required to characterise the

496 observed spatiotemporal extent of groundwater emergence during a flood event and the relationship

497 with both standardized and absolute borehole levels. With previous SPI-like approaches developed

498 for flood warning (Alfieri *et al.*, 2014), such a ground-truthing exercise would be required before the

499 SGFI could be used operationally.

500

501 In this study, we used IRF models for each cluster to determine the relative significance of spatial

502 variations in rainfall input and aquifer properties. This approach could be extended by using spatially

503 coherent rainfall and PET sequences as inputs into distributed groundwater models. This would give

504 indications of the spatial variability in the groundwater flood response at a finer resolution than using

505 single point IRF models. Recent work has shown the SPI to be a poor proxy for the SGI under drought

506 conditions, with numerous false alarms and low drought hit rate (Musuuza *et al.*, 2016). It is likely

507 that a similar relationship between the SPI and the SGFI, developed in this study, will occur. Further

508 work comparing the SGFI with other indices (e.g. the positive part of a non-seasonally normalised SPI,

509 soil moisture, potential evapotranspiration, SPEI) would be helpful.

510

511

512 ## 5   Conclusions

513

514

515 This study has developed a novel approach for regional scale analysis of the spatiotemporal controls

516 on groundwater flooding using statistical analysis of standardized groundwater level hydrographs and

517 IRF modelling. We conclude that there are two spatially coherent SGFI clusters within the southern

518 Chalk of the UK (Group 1 – Wessex and the South Downs, Group 2 – Chilterns) with different rainfall

519 response times. Response times are controlled primarily by the underlying catchment hydrogeology,

520 in particular the extent of the relatively low permeability superficial deposits of Clay-with-Flints and

521 till, which are extensive in Group 2. Groundwater levels were higher during the 2013/14 flood event

522 in Group 1, compared with Group 2, which is reflected in the spatial distribution of groundwater flood

523 impacts collated as part of this study. Modelling indicates that, assuming uniform meteorological

524 conditions across the region, groundwater flooding in 2013/14 in Group 2 may have lasted longer than

525 in Group 1. In general, hydrogeological property variability, in addition to variations in rainfall inputs

526 and antecedent conditions, control the groundwater flood response across the Chalk. This complex

527 combination of controls should be accounted for when managing future groundwater flooding. The

528 approach developed in this study is generic and can be easily applied where long term rainfall and

529 groundwater level data are available.

530

531

532

6 List of Figures

534

535
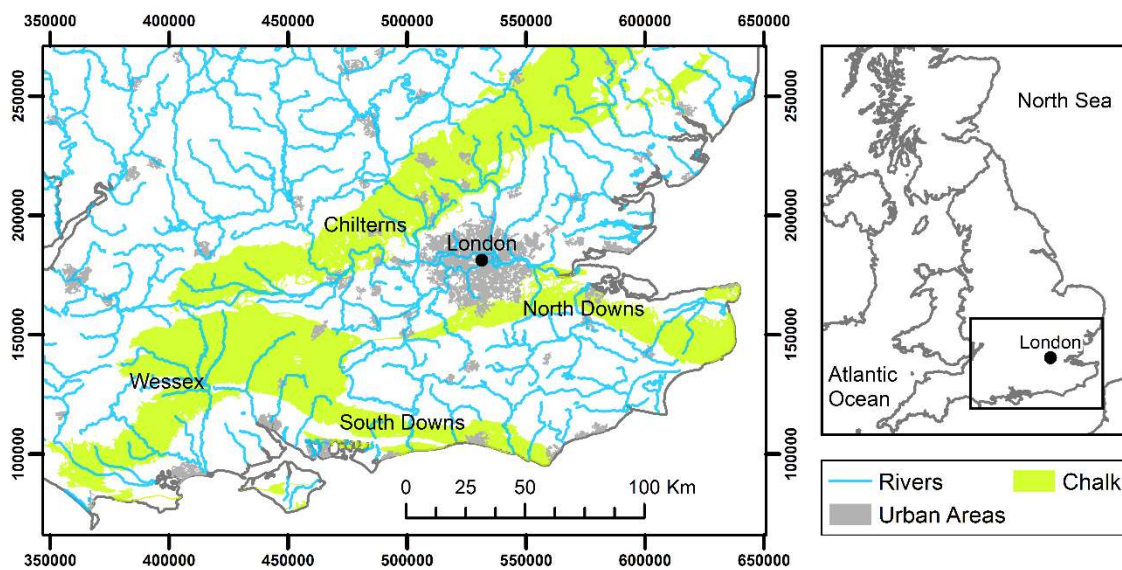
537 **Figure 1: Location of the Chalk outcrop and principal regions in the southern United Kingdom. Contains Ordnance Survey**
538 **data © Crown copyright and database right (2017)**

22

539

540

541

542

543

544

545

546

547

548

549

550
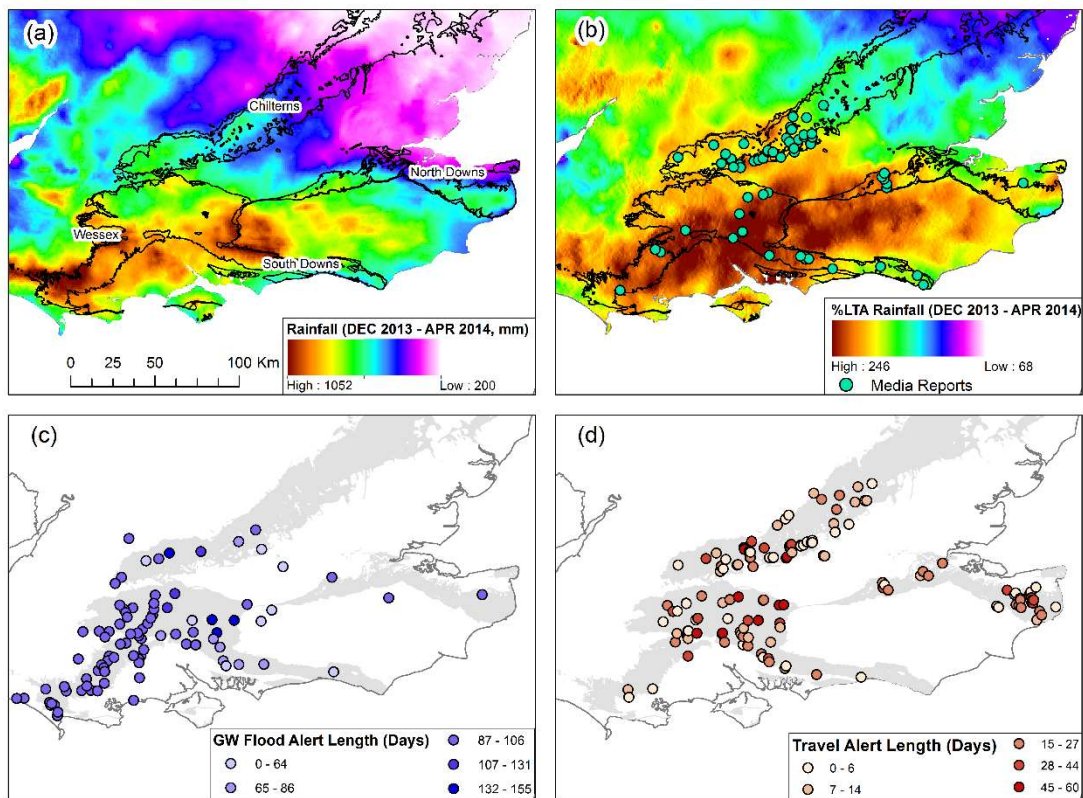
Figure 2: Datasets associated with the flood event of 2013/14 in the southern UK. (a) total winter rainfall (mm) derived from Tanguy *et al.* (2016), (b) total winter rainfall as percentage long term average (%LTA) for 1961 – 2015 and groundwater flood media reports, (c) groundwater flood alert length,(d) travel alert length, . The chalk outcrop is shown in black outline (a – b) and grey (c – d). Contains Ordnance Survey data © Crown copyright and database right (2017) and Environment Agency data © copyright and database right 2015. CEH Gridded Estimates of Areal Rainfall (CEH - GEAR) data licensed from NERC – Centre for Ecology & Hydrology. © Database Right/Copyright NERC – Centre for Ecology & Hydrology. All rights reserved. Contains material based on Met Office data © Crown copyright.

558
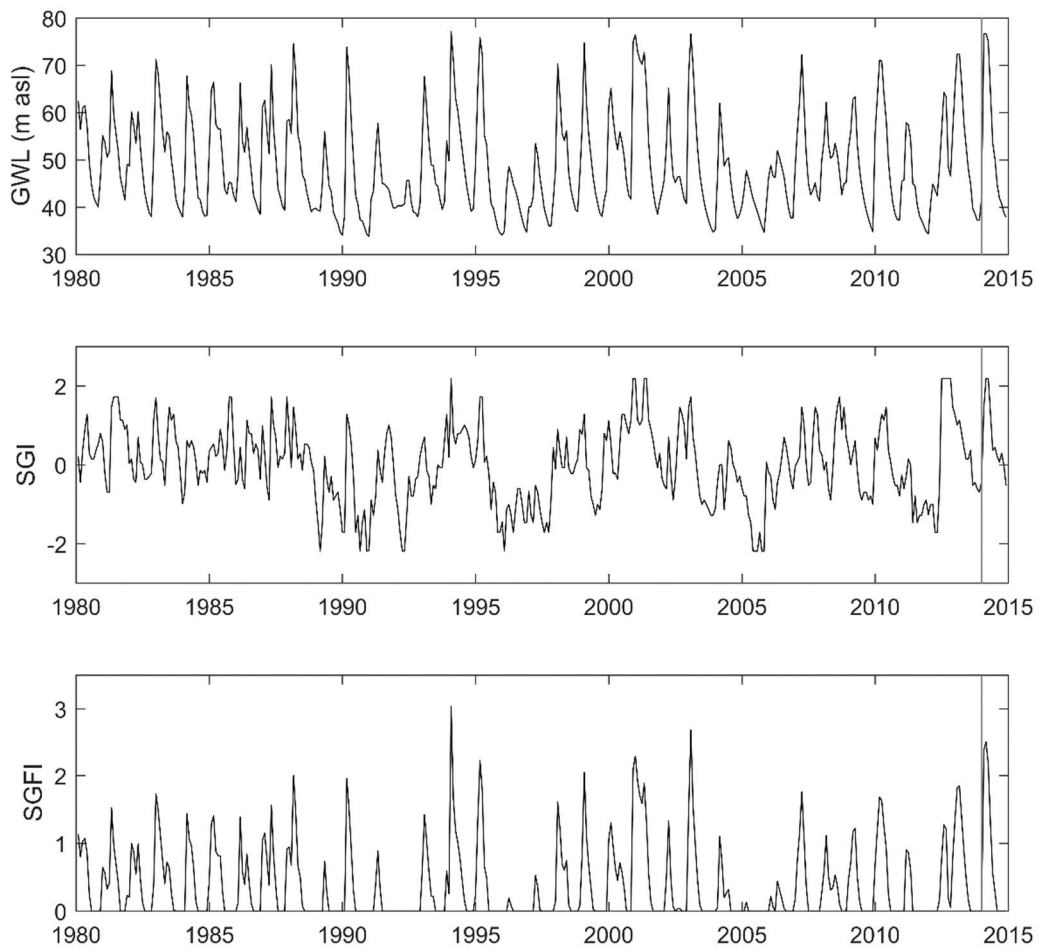
559

563

564
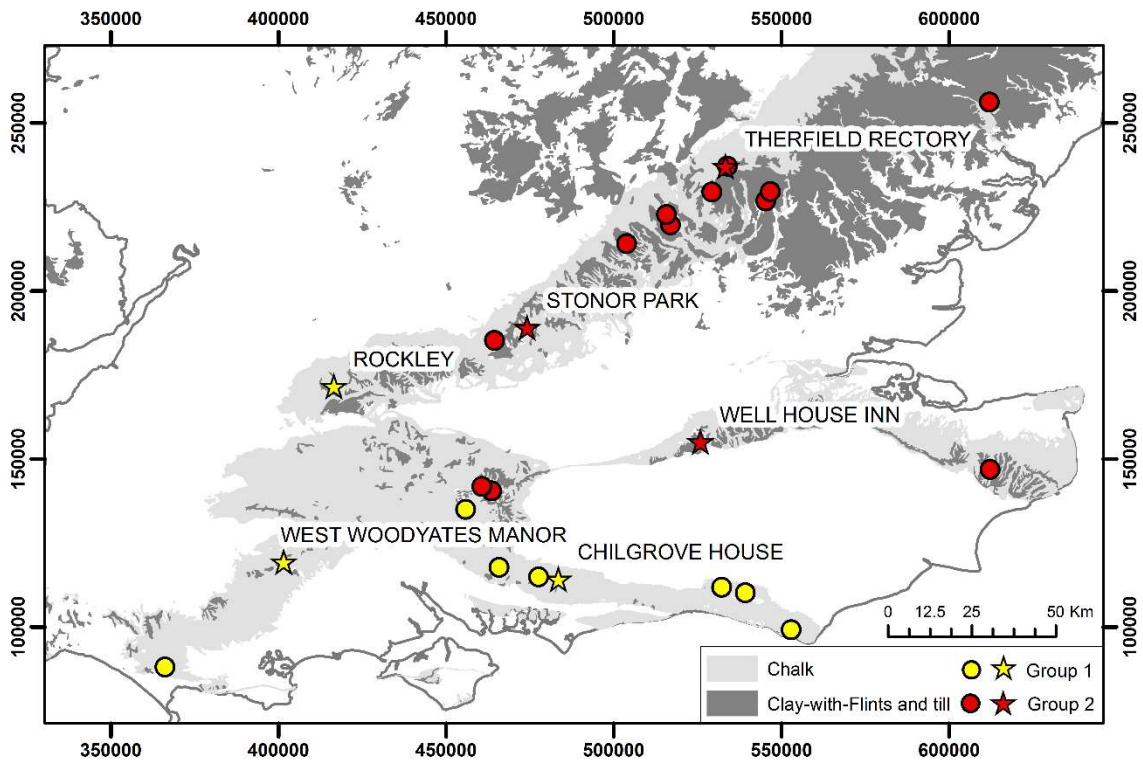
Figure 4: Location of boreholes within the two clusters and the overlaying Clay-with-Flints and till. Boreholes used for IRF modelling are labelled and marked with a star symbol. Contains Ordnance Survey data © Crown copyright and database right (2017).

568

569
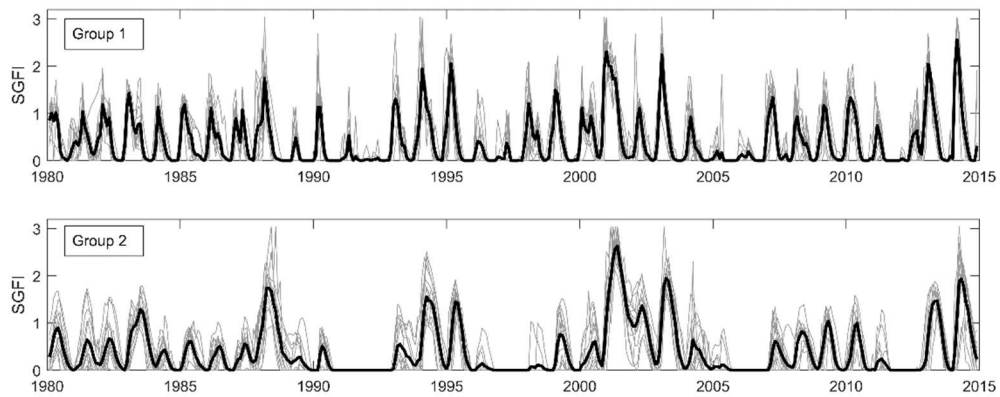
Figure 5: The SGFI for each borehole (grey), divided according to cluster, and the SGFI centroid for each cluster (black)

572

573
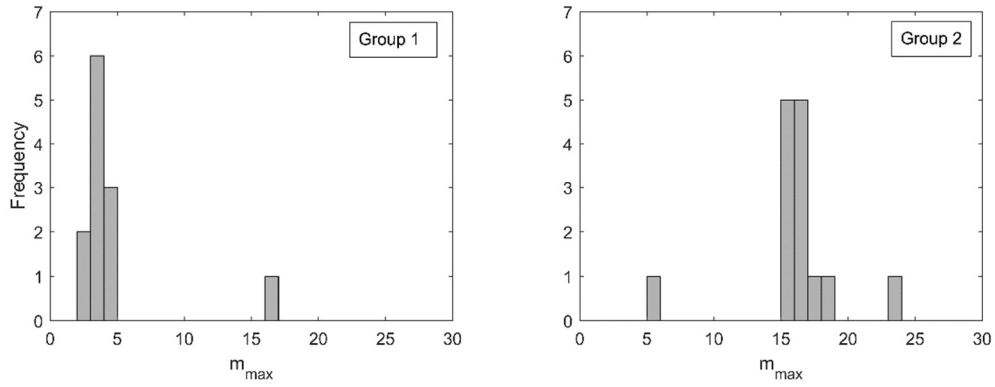
Figure 6: Histograms of the m_{max} value for each borehole divided according to SGFI clustering group.

575

576

577
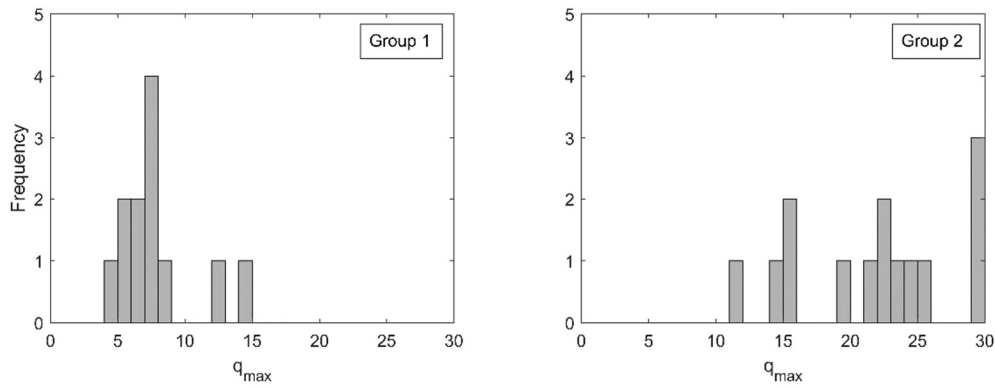
Figure 7: Histograms of the q_{max} value for each borehole divided according to SGFI clustering group.

579

580

581
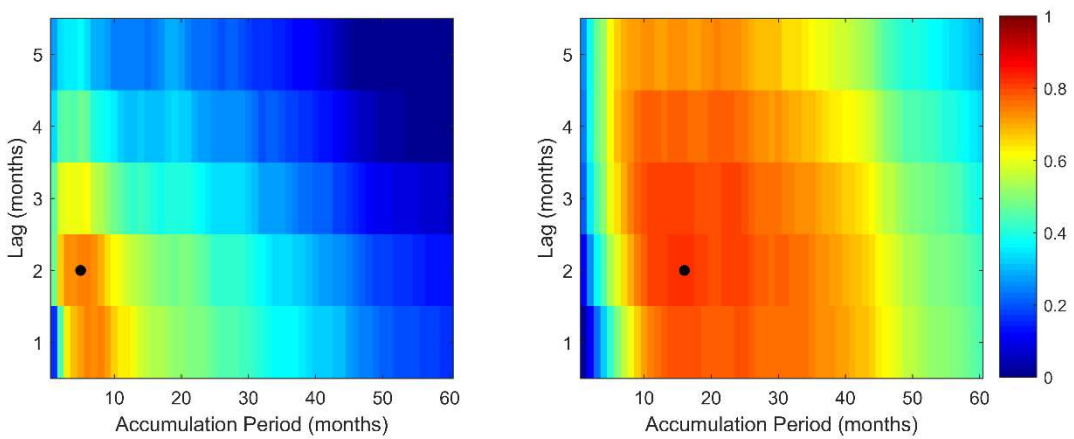
Figure 8: The average correlation between SPI and SGFI for different rainfall accumulation periods and lags for (a) Group 1 and (b) Group 2. The black spot indicates the largest correlation.

584
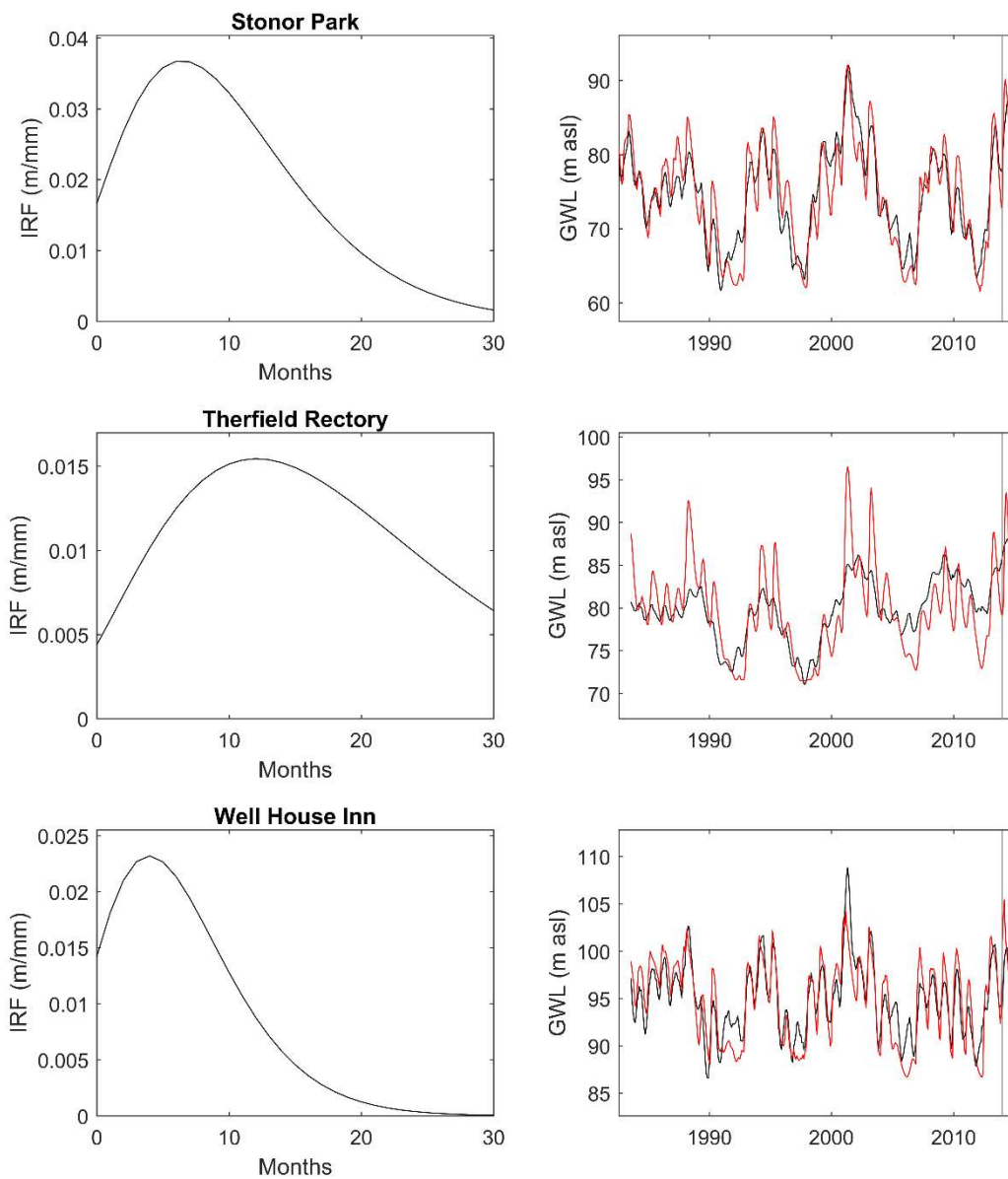
585

586 **Figure 9: IRFs and modelled (black) and observed (red) groundwater levels for sites in Group 1. Grey vertical lines indicate**
587 **1 January 2014. Incorporates data from the UK National Groundwater Level Archive, including water level measurements**
588 **made by the Environment Agency.**

27
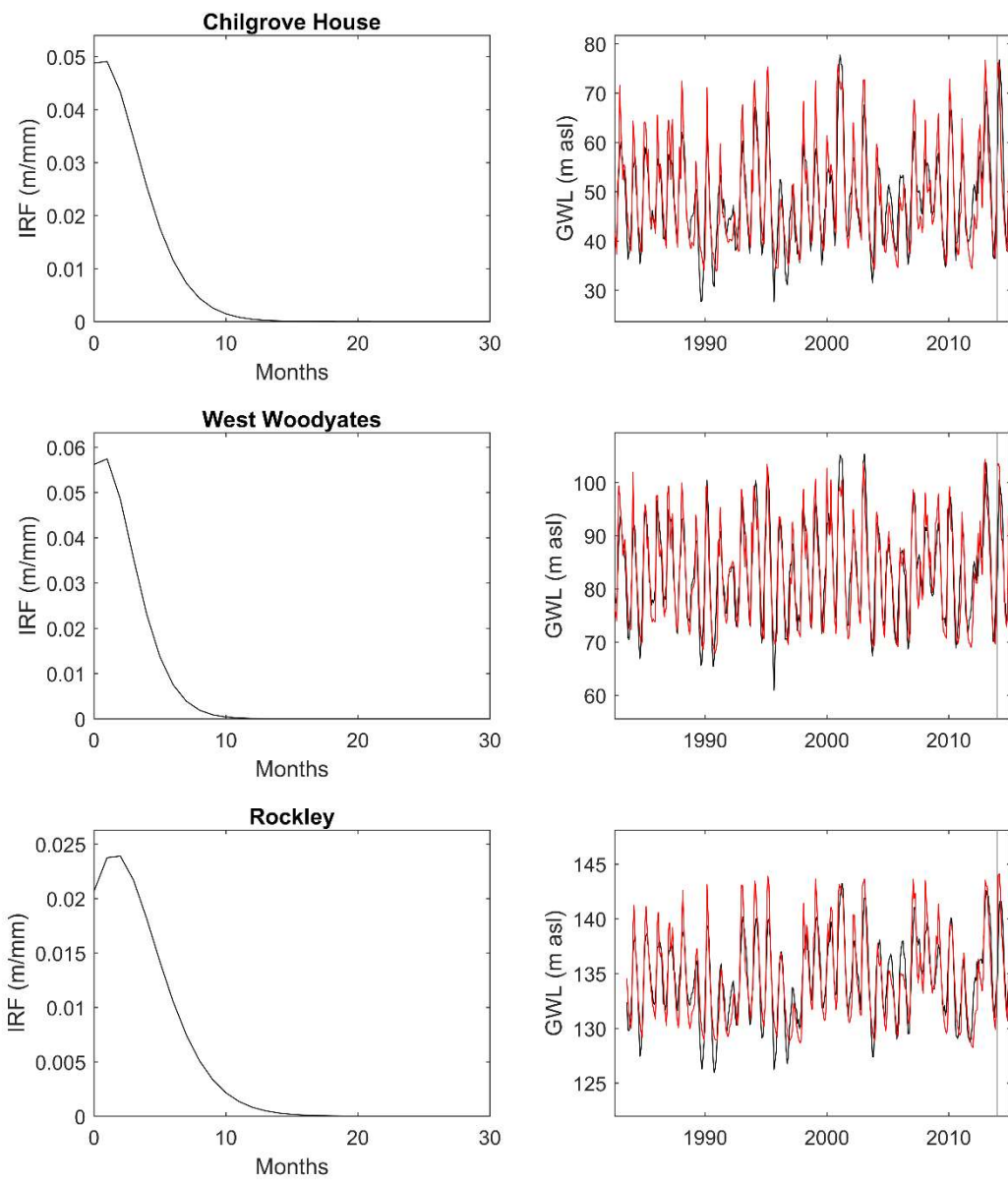
589

590 **Figure 10: IRFs and modelled (black) and observed (red) groundwater levels for sites in Group 2. Grey vertical lines indicate**
591 **1 January 2014. Incorporates data from the UK National Groundwater Level Archive, including water level measurements**
592 **made by the Environment Agency.**

593

594

595

596

Table 1 Range of significant temporal autocorrelation of SGFI ($m_{\max}$) and percentage of Clay-with-Flints and till cover for boreholes in the clusters used for IRF modelling. Model NSE values and the ratio of site rainfall to Chilgrove House rainfall are also shown. Observed and modelled months above 95th percentile level during the 2013/14 flood event using site-specific rainfall and homogeneous rainfall inputs (Chilgrove House) are shown the final three columns.

Group	Site	m_{max}	%CWF and TILL	NSE	Site rainfall / Chilgrove House rainfall	Months above 95th percentile		
						Observed	Modelled (site rainfall)	Modelled (Chilgrove House rainfall)
1	Chilgrove House	3	1	0.76	1	4	7	7
	Rockley	3	6	0.80	0.58	3	5	6
	West Woodyates	2	10	0.82	0.68	3	8	7
2	Stonor Park	16	23	0.82	0.65	6	5	12
	Therfield Rectory	17	86	0.52	0.36	2	16	12
	Well House Inn	16	23	0.72	0.57	3	0	11

8   Acknowledgements

9   References

Adams B, Bloomfield J, Gallagher A, Jackson C, Rutter H, Williams A. 2008. FLOOD 1. Final Report. British Geological Survey, pp: 75.

Adams B, Bloomfield J, Gallagher A, Jackson C, Rutter H, Williams A. 2010. An early warning system for groundwater flooding in the Chalk. Quarterly Journal of Engineering Geology and Hydrogeology, **43**: 185-193.

Alfieri L, Pappenberger F, Wetterhall F. 2014. The extreme runoff index for flood early warning in Europe. Natural Hazards and Earth System Sciences, **14**: 1505-1515.

Allen D, Brewerton L, Coleby L, Gibbs B, Lewis M, MacDonald A, Wagstaff S, Williams A. 1997. The physical properties of major aquifers in England and Wales. British Geological Survey, pp: 333.

Ascott MJ, Lapworth DJ, Gooddy DC, Sage RC, Karapanos I. 2016. Impacts of extreme flooding on riverbank filtration water quality. Science of The Total Environment, **554–555**: 89-101. DOI: http://dx.doi.org/10.1016/j.scitotenv.2016.02.169.

Bloomfield J, Bricker S, Newell A. 2011. Some relationships between lithology, basin form and hydrology: a case study from the Thames basin, UK. Hydrological Processes, **25**: 2518-2530.

Bloomfield J, Marchant B, Bricker S, Morgan R. 2015. Regional analysis of groundwater droughts using hydrograph classification. Hydrology and Earth System Sciences, **19**: 4327-4344.

Bloomfield JP, Allen DJ, Griffiths KJ. 2009. Examining geological controls on baseflow index (BFI) using regression analysis: An illustration from the Thames Basin, UK. Journal of Hydrology, **373**: 164-176. DOI: http://dx.doi.org/10.1016/j.jhydrol.2009.04.025.

Bloomfield JP, Marchant BP. 2013. Analysis of groundwater drought building on the standardised precipitation index approach. Hydrol. Earth Syst. Sci., **17**: 4769-4787. DOI: 10.5194/hess-17-4769-2013.

Blundell DJ. 2002. Cenozoic inversion and uplift of southern Britain. Geological Society, London, Special Publications, **196**: 85-101. DOI: 10.1144/gsl.sp.2002.196.01.06.

Bonacci O, Ljubenkov I, Roje-Bonacci T. 2006. Karst flash floods: an example from the Dinaric karst (Croatia). Nat. Hazards Earth Syst. Sci., **6**: 195-203. DOI: 10.5194/nhess-6-195-2006.

Bricker S, Bloomfield J. 2014. Controls on the basin-scale distribution of hydraulic conductivity of superficial deposits: a case study from the Thames Basin, UK. Quarterly Journal of Engineering Geology and Hydrogeology, **47**: 223-236.

Butler A, Hughes A, Jackson C, Ireson A, Parker S, Wheater H, Peach D. 2012. Advances in modelling groundwater behaviour in Chalk catchments. Geological Society, London, Special Publications, **364**: 113-127.

CH2MHill. 2015. Upper Lavant Valley Flood Risk Management Study. West Sussex County Council, pp: 88.

Chebanov O, Zadniprovska A. 2011. Zoning groundwater flooding risks in the cities and urban agglomeration areas of Ukraine. In: Bloeschl G (Ed.) IAHS, pp: 71-76.

Christensen JH, Christensen OB. 2003. Climate modelling: severe summertime flooding in Europe. Nature, **421**: 805-806.

Cobby D, Morris S, Parkes A, Robinson V. 2009. Groundwater flood risk management: advances towards meeting the requirements of the EU floods directive. Journal of Flood Risk Management, **2**: 111-119. DOI: 10.1111/j.1753-318X.2009.01025.x.

Davies HC. 2015. Weather chains during the 2013/2014 winter and their significance for seasonal prediction. Nature Geosci, **8**: 833-837. DOI: 10.1038/ngeo2561

http://www.nature.com/ngeo/journal/v8/n11/abs/ngeo2561.html#supplementary-information.

Downing RA, Price M, Jones GP. 1993. The hydrogeology of the Chalk of north-west Europe., Clarendon Press.

Environment Agency. 2015. WFD River Waterbody Catchments Cycle 2. https://data.gov.uk/dataset/wfd-river-waterbody-catchments-cycle-2.

Environment Agency. 2016. The costs and impacts of the winter 2013 to 2014 floods. Environment Agency.

ESI. 2016. £530m: The Hidden Economic Cost of Groundwater Flooding Revealed. http://esi-consulting.co.uk/530m-hidden-economic-cost-groundwater-flooding-revealed/.

ESI. 2016. ESI Launches Ground-Breaking 5 Metre Groundwater Flood Risk Map. http://esi-consulting.co.uk/esi-launches-ground-breaking-5-metre-groundwater-flood-risk-map/.

Finch JW, Bradford RB, Hudson JA. 2004. The spatial distribution of groundwater flooding in a chalk catchment in southern England. Hydrological Processes, **18**: 959-971. DOI: 10.1002/hyp.1340.

Folland C, Hannaford J, Bloomfield J, Kendon M, Svensson C, Marchant B, Prior J, Wallace E. 2015. Multi-annual droughts in the English Lowlands: a review of their characteristics and climate drivers in the winter half-year. Hydrology and Earth System Sciences, **19**: 2353-2375.

Fowler HJ, Ekström M. 2009. Multi-model ensemble estimates of climate change impacts on UK seasonal precipitation extremes. International Journal of Climatology, **29**: 385-416. DOI: 10.1002/joc.1827.

Fürst J, Bichler A, Konecny F. 2015. Regional frequency analysis of extreme groundwater levels. Groundwater, **53**: 414-423.

Gotkowitz MB, Attig JW, McDermott T. 2014. Groundwater flood of a river terrace in southwest Wisconsin, USA. Hydrogeology Journal, **22**: 1421-1432. DOI: 10.1007/s10040-014-1129-x.

Hannaford J, Muchan K, Lewis MA, Clemas S. 2014. Hydrological summary for the United Kingdom: January 2014. Centre for Ecology & Hydrology, pp: 12.

Hough M, Jones R. 1999. The United Kingdom Meteorological Office rainfall and evaporation calculation system: MORECS version 2.0-an overview. Hydrology and Earth System Sciences, **1**: 227-239.

Hughes A, Vounaki T, Peach D, Ireson A, Jackson C, Butler A, Bloomfield J, Finch J, Wheater H. 2011. Flood risk from groundwater: examples from a Chalk catchment in southern England. Journal of Flood Risk Management, **4**: 143-155.

Huntingford C, Marsh T, Scaife AA, Kendon EJ, Hannaford J, Kay AL, Lockwood M, Prudhomme C, Reynard NS, Parry S, Lowe JA, Screen JA, Ward HC, Roberts M, Stott PA, Bell VA, Bailey M, Jenkins A, Legg T, Otto FEL, Massey N, Schaller N, Slingo J, Allen MR. 2014. Potential influences on the United Kingdom's floods of winter 2013/14. Nature Clim. Change, **4**: 769-777. DOI: 10.1038/nclimate2314.

Huntingford C, Marsh T, Scaife AA, Kendon EJ, Hannaford J, Kay AL, Lockwood M, Prudhomme C, Reynard NS, Parry S, Lowe JA, Screen JA, Ward HC, Roberts M, Stott PA, Bell VA, Bailey M, Jenkins A, Legg T, Otto FEL, Massey N, Schaller N, Slingo J, Allen MR. 2015. Reply to 'Drivers of the 2013/14 winter floods in the UK'. Nature Clim. Change, **5**: 491-492. DOI: 10.1038/nclimate2613.

Ireson AM, Butler AP. 2011. Controls on preferential recharge to Chalk aquifers. Journal of Hydrology, **398**: 109-123. DOI: http://dx.doi.org/10.1016/j.jhydrol.2010.12.015.

JBA. 2016. JBA launches national groundwater flood map. http://www.jbaconsulting.com/news/jba-launches-national-groundwater-flood-map.

Jimenez-Martinez J, Smith M, Pope D. 2016. Prediction of groundwater-induced flooding in a chalk aquifer for future climate change scenarios. Hydrological Processes, **30**: 573-587. DOI: 10.1002/hyp.10619.

Kendon M, McCarthy M. 2015. The UK's wet and stormy winter of 2013/2014. Weather, **70**: 40-47. DOI: 10.1002/wea.2465.

Klinck BA, Hopson P, Lewis MA. 1988. The Hydrogeological Behaviour of the Clay-With-Flints of Southern England. British Geological Survey.

716   Klinck BA, Hopson P, Morigi AN, Bloodworth AJ, Inglethorpe SDJ, Entwisle DC, Wealthall GP. 1997.
717   The Hydrogeological Classification of Superficial Clay: The hydrogeology characterisation of
718   glacial till in East Anglia. British Geological Survey.

719   Kreibich H, Thieken A, Grunenberg H, Ullrich K, Sommer T. 2009. Extent, perception and mitigation
720   of damage due to high groundwater levels in the city of Dresden, Germany. Natural Hazards
721   and Earth System Sciences, **9**: 1247-1258.

722   Lee LJE, Lawrence DSL, Price M. 2006. Analysis of water-level response to rainfall and implications
723   for recharge pathways in the Chalk aquifer, SE England. Journal of Hydrology, **330**: 604-620.
724   DOI: http://dx.doi.org/10.1016/j.jhydrol.2006.04.025.

725   MacDonald AM, Allen DJ. 2001. Aquifer properties of the Chalk of England. Quarterly Journal of
726   Engineering Geology and Hydrogeology, **34**: 371-384. DOI: 10.1144/qjegh.34.4.371.

727   Macdonald D, Dixon A, Newell A, Hallaways A. 2012. Groundwater flooding within an urbanised
728   flood plain. Journal of Flood Risk Management, **5**: 68-80.

729   Macdonald DMJ, Bloomfield JP, Hughes A, MacDonald AM, Adams B, McKenzie AA. 2008. Improving
730   the understanding of the risk from groundwater flooding in the UK. CRC Press.

731   Mackay J, Jackson C, Brookshaw A, Scaife A, Cook J, Ward R. 2015. Seasonal forecasting of
732   groundwater levels in principal aquifers of the United Kingdom. Journal of Hydrology, **530**:
733   815-828.

734   Mackay J, Jackson C, Wang L. 2014. A lumped conceptual model to simulate groundwater level time-
735   series. Environmental Modelling & Software, **61**: 229-245.

736   Marchant B, Mackay J, Bloomfield J. 2016. Quantifying uncertainty in predictions of groundwater
737   levels using formal likelihood methods. Journal of Hydrology, **540**: 699-711. DOI:
738   http://dx.doi.org/10.1016/j.jhydrol.2016.06.014.

739   McKee TB, Doesken NJ, Kleist J. 1993. The relationship of drought frequency and duration to time
740   scales. In: Proceedings of the 8th Conference on Applied Climatology, American
741   Meteorological Society Boston, MA, pp: 179-183.

742   McKenzie A, Rutter H, Hulbert A. 2010. The use of elevation models to predict areas at risk of
743   groundwater flooding. Geological Society, London, Special Publications, **345**: 75-79.

744   Morris S, Cobby D, Parkes A. 2007. Towards groundwater flood risk mapping. Quarterly Journal of
745   Engineering Geology and Hydrogeology, **40**: 203-211.

746   Morris SE, Cobby D, Zaidman M, Fisher K. 2015. Modelling and mapping groundwater flooding at the
747   ground surface in Chalk catchments. Journal of Flood Risk Management. DOI:
748   10.1111/jfr3.12201.

749   Muchan K, Lewis M, Hannaford J, Parry S. 2015. The winter storms of 2013/2014 in the UK:
750   hydrological responses and impacts. Weather, **70**: 55-61.

751   Musuuza JL, Van Loon AF, Teuling AJ. 2016. Multiscale evaluation of the standardized precipitation
752   index as a groundwater drought indicator. Hydrology and Earth System Sciences, **20**: 1117.

753   Naughton O, Johnston PM, McCormack T, Gill LW. 2015. Groundwater flood risk mapping and
754   management: examples from a lowland karst catchment in Ireland. Journal of Flood Risk
755   Management. DOI: 10.1111/jfr3.12145.

756   Peters E, Torfs P, Van Lanen H, Bier G. 2003. Propagation of drought through groundwater—a new
757   approach using linear reservoir theory. Hydrological processes, **17**: 3023-3040.

758   Pinault JL, Amraoui N, Golaz C. 2005. Groundwater-induced flooding in macropore-dominated
759   hydrological system in the context of climate changes. Water Resources Research, **41**: n/a-
760   n/a. DOI: 10.1029/2004WR003169.

761   Pirazzoli PA, Costa S, Dornbusch U, Tomasin A. 2006. Recent evolution of surge-related events and
762   assessment of coastal flooding risk on the eastern coasts of the English Channel. Ocean
763   Dynamics, **56**: 498-512. DOI: 10.1007/s10236-005-0040-3.

764   Robinson VK, Solomon J, Morris S. 2001. Groundwater Flooding in the Thames Region, Winter
765   2000/01. Environment Agency.

766 Schaller N, Kay AL, Lamb R, Massey NR, van Oldenborgh GJ, Otto FEL, Sparrow SN, Vautard R, Yiou P,
767   Ashpole I, Bowery A, Crooks SM, Haustein K, Huntingford C, Ingram WJ, Jones RG, Legg T,
768   Miller J, Skeggs J, Wallom D, Weisheimer A, Wilson S, Stott PA, Allen MR. 2016. Human
769   influence on climate in the 2014 southern England winter floods and their impacts. Nature
770   Clim. Change, **6**: 627-634. DOI: 10.1038/nclimate2927

771 http://www.nature.com/nclimate/journal/v6/n6/abs/nclimate2927.html#supplementary-
772   information.
773 South Oxfordshire District Council. 2016. Borehole data from Stonor Park.
774   http://www.southoxon.gov.uk/services-and-advice/environment-and-neighbourhood-
775   issues/severe-weather/flooding/borehole-data-stono.
776 Tanguy M, Dixon H, Prosdocimi I, Morris DG, Keller VDJ. 2016. Gridded estimates of daily and
777   monthly areal rainfall for the United Kingdom (1890-2015) [CEH-GEAR]. NERC Environmental
778   Information Data Centre.
779 Tijdeman E, Bachmair S, Stahl K. 2016. Controls on hydrologic drought duration in near-natural
780   streamflow in Europe and the USA. Hydrol. Earth Syst. Sci., **20**: 4043-4059. DOI:
781   10.5194/hess-20-4043-2016.
782 United Nations Office for Disaster Risk Reduction. 2013. 2013 floods a "turning point".
783   https://www.unisdr.org/archive/33693.
784 Upton KA, Jackson CR. 2011. Simulation of the spatio-temporal extent of groundwater flooding using
785   statistical methods of hydrograph classification and lumped parameter models. Hydrological
786   Processes, **25**: 1949-1963. DOI: 10.1002/hyp.7951.
787 Van Lanen HAJ, Wanders N, Tallaksen LM, Van Loon AF. 2013. Hydrological drought across the
788   world: impact of climate and physical catchment structure. Hydrol. Earth Syst. Sci., **17**: 1715-
789   1732. DOI: 10.5194/hess-17-1715-2013.
790 Van Loon AF, Laaha G. 2015. Hydrological drought severity explained by climate and catchment
791   characteristics. Journal of Hydrology, **526**: 3-14. DOI:
792   http://dx.doi.org/10.1016/j.jhydrol.2014.10.059.
793 van Oldenborgh GJ, Stephenson DB, Sterl A, Vautard R, Yiou P, Drijfhout SS, von Storch H, van den
794   Dool H. 2015. Drivers of the 2013/14 winter floods in the UK. Nature Clim. Change, **5**: 490-
795   491. DOI: 10.1038/nclimate2612

796 http://www.nature.com/nclimate/journal/v5/n6/abs/nclimate2612.html#supplementary-
797   information.
798 von Asmuth JR, Bierkens MFP, Maas K. 2002. Transfer function-noise modeling in continuous time
799   using predefined impulse response functions. Water Resources Research, **38**: 23-21-23-12.
800   DOI: 10.1029/2001WR001136.
801 Webster R, Oliver MA. 1990. Statistical methods in soil and land resource survey. Oxford University
802   Press (OUP).
803 Wu H, Adler RF, Hong Y, Tian Y, Policelli F. 2012. Evaluation of global flood detection using satellite-
804   based rainfall and a hydrologic model. Journal of Hydrometeorology, **13**: 1268-1284.
805 Yevyevich V. 1967. An Objective Approach to Definition and Investigations of Continental Hydraulic
806   Droughts. Colorado State University.

807